Extended EDC local extinction model accounting finite-rate chemistry for MILD combustion

Javad Aminian[1,†], Chiara Galletti[2], Leonardo Tognotti[2]

[1] *Mechanical and Energy Engineering Department, Shahid Beheshti University, Tehran - IRAN*

[2] *Civil and Industrial Engineering Department, University of Pisa, Pisa - ITALY*

Abstract An extended Eddy Dissipation Concept (EDC) local extinction model is proposed to take into account the effects of finite-rate chemistry, normally occurred in Moderate to Intense Low oxygen Dilution (MILD) combustion, on the extinction limits. Local extinction is predicted when the local fine structure residence time is below a local critical value that is determined theoretically in the present study. The proposed model has been evaluated against experimental data reported for CH_4/H_2 jet-in-hot and diluted coflow flames. Comparison with the standard EDC extinction model is also presented. Results show that prediction of extinction threshold in MILD conditions is attainable only through the application of the extended EDC extinction model on a well resolved turbulence-chemistry interaction field. The effect of penetrating of surrounding air into the reaction zone and subsequent flame cooling at downstream is also captured by the proposed extinction model. Despite its simplicity, the extended EDC extinction model describes many features of localized extinction under the MILD combustion as well as conventional combustion conditions.

Keywords: *Extinction model; flameless combustion; turbulent jets; diffusion flames; finite-rate chemistry effects; numerical analysis*

[†] Corresponding Author: Phone: +98 021 73 93 2693, Fax: +98 21 77 31 1446
E-mail: j_aminian@sbu.ac.ir

1 Introduction

A good understanding of the phenomena governing the extinction of turbulent diffusion flames is essential because of their widespread appearance in practical combustion applications. A large amount of experiments in jet diffusion flames using a variety of laser techniques revealed that local extinction may occur in two physical and chemical stages [1]. In a coflow jet diffusion flame studied by Takahashi et al. [2], these stages were found to be related to the unsteady transport effects of external or internal vortices on chemical kinetics. Detailed experiments of Rolon et al. [3] on a counter flow diffusion flame showed that the strong vortices were responsible of flame extinction and subsequent blowout while re-ignition occurred after interaction with weak vortices. Kim et al. performed a comprehensive study on the effect of strain rate and conductive heat loss on the premixed and partially premixed syngas-air flames extinction [4]. They investigated various mechanisms responsible for flame extinction and showed that the lower and upper extinction boundaries as well as reaction zone thickness can become narrower with increasing strain rate. By the analysis of flame structure near extinction on CH_4, H_2, H_2/Ar, and $CO/H_2/N_2$ jet diffusion flames, Masri et al. [5, 6] revealed that extinction is only slightly affected by turbulence and is mainly controlled by the width of the reaction zone. For instance, addition of methane to fuel promoted local extinction as it reduces the width of reaction zone due to scavenging reactive radical species like H and OH. Based on the comprehensive set of measurements of the local flame structure provided by Masri et al. [5, 6], Koutmos developed a local critical Damkohler number criterion to determine extinction limits in turbulent methane jet diffusion flames [7].

As presented above, various studies are being attempted worldwide to investigate the governing concepts of flame extinction under conventional premixed or diffusion combustion regimes. However, for innovative combustion technologies such as the Moderate or Intense Low-oxygen Dilution (MILD) combustion, phenomena which control extinction may be different due to the strong differences in kinetics and flow fields with respect to conventional combustion. In MILD combustion, the fuel is burnt with a highly diluted oxidant supplied at a temperature higher than the reacting mixture self-ignition temperature. Spontaneous ignition occurs and progresses with no visible or audible signs of the flames usually associated with conventional combustion. In this regime the diffusing and broaden reaction zone leads to almost uniform heat release and smooth temperature field. These features results in a much more efficient combustion as well as in a suppression of pollutant emissions [8]. This technology is also known as flameless combustion due to its invisible flame front [9] and high temperature air combustion (HiTAC) due to the common procedure of preheating the oxidizer to ensure the mixture temperature to be higher than the self-ignition temperature [10].

A few works discussed the extinction behavior in MILD combustion, partly with the aim to elucidate the role of governing parameters on the extinction limits. Mastorakos et al. [11] investigated the effects of simultaneous dilution and preheating of reactants by mixing with hot combustion products in terms of the stability of turbulent counter flow flames. The air was heated from ambient temperature up to 1750 K while it was diluted down to 0.02 mole fraction of oxygen. Extinction limits were measured by igniting the flame under stable conditions and gradually increasing the bulk velocity or decreasing the oxygen content until the flame was extinguished. They concluded that a temperature

increase of 100 K is necessary for every 0.02 mole fraction of oxygen loosed by dilution to maintain stability. Flame instabilities were observed for air temperatures less than 1400 K. They reported that dilution level of vitiated air did not affect the extinction of lean premixed flames. Its temperature, however, was indicated as the main parameter affecting the transition from sudden extinction to no-extinction regime [10, 11].

Maruta et al. carried out an experimental study on a counter flow burner fed with N_2-diluted methane and air with temperature between 300 to 800 K to study the combustion limit and reaction zone structure in flameless combustion regime [12]. One-dimensional computation with detailed chemistry was also performed to cover a wider air temperature range. Similar to Mastorakos et al. they reported that when the air temperature was kept higher than 1300 K, extinction limits disappeared. In this temperature range, combustion continues even under extremely fuel-lean conditions such as 1% methane in nitrogen since the energy that high temperature air brings into the reaction zone is high enough to sustain a weak reaction zone [11, 12].

Kumar et al. proposed an empirical flame extinction model based on the competition between mixing and chemical time-scales to predict extinction limits and flame lift-off height in MILD combustion conditions [13]. The extinction model which accounted for reactants dilution and preheating of the oxidizer was evaluated against flame lift-off height for a variety of experiments reported in the literatures [13, 14].

Very recently, Lilleberg et al. [15] conducted a numerical study using the EDC combustion model with a pre-calculated extinction database using single and two-step chemical mechanisms on the Sandia/TNF Flame D and Flame E. For the local extinction approach a database of chemical time scales for different inlet temperatures (300 to 865

K) and equivalence ratios (about zero to 5) was pre-calculated based on the well-stirred reactor assumption. Similar to the Kumar's approach, Lilleberg et al. [15] assumed that if the fine structure residence time was lower than the pre-calculated chemical time-scales extinction occurs. They compared results of the local extinction approach with a fast-chemistry EDC approach known as the Eddy Dissipation Model and a full detailed chemical mechanism of the gas research institute (GRI-Mech 3.0) and showed that the detailed chemistry approach gave the best predictions compared to the experiments with a considerable higher calculation efforts compared to the fast chemistry and local extinction approaches.

In MILD combustion, accurate treatment of turbulence-chemistry interaction (TCI) through a proper combustion model plays a fundamental role for modeling and predicting this regime. Most works have highlighted the superior performances of the Eddy Dissipation Concept (EDC) [16-18] combustion model with respect to others, mainly because such a model allows taking into account finite-rate chemistry effects and an efficient implementation of detailed kinetics. However, some researchers showed that the EDC combustion model usually over-predicts the flame temperature for MILD conditions, so both Aminian et al. [19] and De et al. [20] suggested a revision of the model for MILD conditions, based on an increase of the EDC fine structure residence time constant. The importance of combustion model on capturing the interaction between chemical oxidation and turbulence are also emphasized by Duwig and Dunn [21] for Jet-in-Hot Coflow (JHC) with highly turbulent shear layers.

The present study is aimed at developing a new extinction model applicable for MILD combustion conditions and at further characterizing the importance of accurate treatment of the turbulence-chemistry interaction towards local extinction analysis.

2 Experimental observations

The Jet-in-Hot Coflow burner experimentally studied by Dally et al. [22] consists of a central fuel jet (i.d. = 4.25 mm) which is surrounded coaxially by an annulus (i.d. = 82 mm) equipped with a secondary burner providing hot combustion products (Fig. 1). The hot flue gases are premixed with air and nitrogen via two side-inlets at the bottom of the annulus to vitiate the oxidizer and produce coflow streams with 9%, 6% and 3% oxygen mass fraction denoted as HM3, HM2, and HM1 flames, respectively. The whole burner was placed inside a wind tunnel, with room temperature air at the same velocity as the hot coflow, to help the stabilization of the flames. In this research the HM3 and HM1 flames are interested as they mimic characterization of the diffusion-like flames as well as the MILD conditions, respectively.

Using the scatter data for hydroxyl radical (OH), Dally et al. [22] reported that no sign of localized extinction was observed at upstream (z < 100 mm) for all JHC flames. However, based on the large scatter of OH around stoichiometric mixture fraction for HM1 flame they concluded that only HM1 flame partly extinguished at the downstream (z = 120 mm). The scatter plots of hydroxyl radical alone, while providing useful insights into the flame structure does not give enough information to fully resolve issues regarding reaction zone structure and local extinction effects. Such issues require additional information; best provided by radical species, such as oxygen and formaldehyde (CH_2O). The hydroxyl radical is, normally, used as a flame marker, while

137 the formaldehyde intermediate species is predominant at low temperatures typical of
138 those found in MILD combustion.

139 Medwell et al. [23] performed a more in-depth analysis of local extinction using the
140 instantaneous images of the OH, CH_2O and temperature on the similar experiment of the
141 JHC burner with slightly higher jet Reynolds number. They reported that at the
142 downstream the entrainment of surrounding air can lead to localized extinction of the
143 reaction zone by means of cooling. They stated that the extinction/re-ignition phenomena
144 in JHC flames occur in a consecutive manner. First, extinction occurs due to cooling by
145 the surrounding air. Then, breaking of the reaction zone leads to premixing of the fuel
146 and surrounding air. Finally, the premixed fuel-air ignites by the heated coflow which
147 acts as a pilot. Employing the OH and temperature images they showed that the
148 associated temperature drop from the surrounding air can lead to localized extinction at
149 downstream for the HM1 flame. However, the entrainment of surrounding air into the
150 HM3 flame with more intense initial reaction zone lead to weaken the reaction zone
151 rather than extinction. In addition, they have reported that physical strained induced
152 mechanisms have no effect on the extinction of JHC flames and the increased frequency
153 of extinction events with the increased Reynolds number was attributed to the increased
154 mixing and entraining more cooling air into the reaction zone. Based on the analysis of
155 the OH, CH_2O and temperature image set at z = 125 mm they showed that 11.9% of HM1
156 flame was extinguished while no extinction was observed for the HM3 flame [23].

157 In another study on the HM1 flame, Medwell et al. demonstrated that different
158 stabilization mechanisms are governed in the MILD conditions [24]. They showed that
159 lower amount of O_2 in the heated coflow lead to lower reaction rates and therefore lower

160 OH concentration which was defined as weakened reaction zone. The non-intense
161 weakened reaction zone subsequently allows more permeation of oxygen across the
162 reaction zone and leads to some partial premixing in the lift-off region. Their observation
163 suggests that molecular transport and finite-rate chemistry effects are essential in order to
164 capture the stability and structure of flames in MILD conditions.

165 The comprehensive set of detailed measurements of Dally et al. [22] and Medwell et
166 al. [23, 24] provides a thorough insight on the local structure of the HM1 and HM3
167 flames and help to identify a set of parameters that control their behavior close to
168 extinction. Based on these findings, a new local extinction criterion will be hereby
169 developed and presented following to the standard EDC extinction model.

170 3 Computational and Physical models

171 Due to the symmetry of the HM1 and HM3 flames, a 2D axisymmetric domain
172 starting from the burner exit was constructed (Fig. 2). A mesh independency task was
173 performed on four structured grids of 13, 20, 25 and 33k elements. Comparing the cold-
174 flow velocity profile along the burner center line the grid with 25k cells was found to be
175 the optimum grid.

176 The steady-state Reynolds-Averaged Navier-Stokes (RANS) equations are solved
177 with a finite volume scheme using the commercial CFD code FLUENT. The modified k-
178 ε turbulence model ($C_{\varepsilon 1}$ is set to 1.6 instead of 1.44) was employed to compensate for the
179 round-jet/plane-jet anomaly [25]. The full KEE58 mechanism [26] consists of 17 species
180 (CH_4, O_2, CH_3, CH_2, CH, CH_2O, HCO, CO_2, CO, H_2, H, O, OH, H_2O, HO_2, H_2O_2, and
181 N_2) and 58 reversible reactions related to methane is employed in this study. Differential
182 diffusion was considered based the kinetic theory and a modification of the Chapman-

Enskog formula [27]. The discrete ordinate (DO) method together with the Weighted-Sum-of-Gray-Gases (WSGG) model was employed to solve the radiative transfer equation (RTE) in 16 different directions across the computational domain. Second-order upwind scheme was applied for discretizing all transport equations and the SIMPLE algorithm to handle velocity-pressure coupling. Table 1 shows the operating conditions of all inlet streams for the HM1 and HM3 flames.

4 Model descriptions

The main focus of this paper is on developing a new extinction model for MILD combustion conditions based on the classical EDC extinction model developed for the conventional diffusion flames. However, every extinction model should be coupled with a combustion model to enjoy the thermo-chemistry and turbulence properties calculated by the combustion model. Therefore, at first the modified EDC combustion model which is previously studied by the authors of this paper will be briefly discussed in section 4.1. Then details of the EDC extinction model will be critically reviewed and an extended extinction model for MILD combustion conditions will be presented in sections 4.2 and 4.3, respectively. Fig. 3 illustrates a conceptual scheme of the modeling strategy performed in the previous studies (STEP 1 and STEP 2: modifying the EDC combustion model constant for MILD conditions) and the overall procedure of developing a new extinction model for MILD conditions in the present paper (STEP 3 to STEP 5).

4.1 EDC combustion model

The EDC combustion model provides an empirical expression for the mean reaction rate based on the assumption that the chemical reactions occur in the regions of the flow which represent only a fraction of the entire volume and where the dissipation of

turbulent kinetic energy takes place [28]. These regions are denoted as fine structures and they are believed to be vortex tubes, sheets or slabs, whose characteristic dimensions are of the same order of the Kolmogorov length scale. Gran and Magnussen [29] proposed an expression for the mean reaction rate of specie *i* in a fine structure as:

$$\bar{R}_i = \frac{\gamma^{*2/3}}{\tau^*}\left(Y_i^* - Y_i^0\right) \tag{1}$$

where, γ^* is the fine structure volume and τ^* is the fine structure residence time. Y_i^0 is the mass fraction of species *i* in the surrounding fluid and Y_i^* is the fine structure species mass fraction after reacting over the time τ^*. From the concept of step-wise turbulence energy cascade, characteristic scales of the fine structure have been introduced in the EDC combustion model as follows:

$$\gamma^* = \left(\frac{3C_{D_2}}{4C_{D_1}}\right)^{3/4}\left(\frac{\nu\varepsilon}{k^2}\right)^{3/4} = C_\gamma\left(\frac{\nu\varepsilon}{k^2}\right)^{3/4} \tag{2}$$

$$\tau^* = \left(\frac{C_{D_2}}{3}\right)^{1/2}\left(\frac{\nu}{\varepsilon}\right)^{1/2} = C_t\left(\frac{\nu}{\varepsilon}\right)^{1/2} \tag{3}$$

where, ν, k and ε are the kinematic viscosity, turbulent kinetic energy and its dissipation rate, respectively. C_{D_1} and C_{D_2} are the model constants set equal to 0.134 and 0.5 leading to fine structure volume and residence time constants equal to $C_\gamma = 2.1637$ and $C_t = 0.4083$.

In recent studies, an increase of the fine structure residence time constant in the EDC combustion model has been suggested for better prediction of the interaction between turbulence and chemistry (TCI) in MILD combustion conditions [19, 20]. Figs. 4 and 5 illustrate the effect of increasing C_t from the default value (i.e., 0.4083) to 1.5 on the

prediction of temperature and hydroxyl profiles obtained with the KEE58 mechanism and the modified k-ε turbulence model for the HM1 and HM3 flames [19].

As can be seen in Figs. 4 and 5, results of the standard EDC combustion model, hereafter called *Std. EDC-TCI*, showed an intensified reaction zone at downstream. However, the modified EDC combustion model (*Mod. EDC-TCI*) accounts for the reaction zone weakening as it reduces the peak values of temperature and hydroxyl radical makes it more reliable for MILD combustion conditions. Some under prediction of OH radical at the upstream of HM1 and HM3 flames is attributed to the unattained temperature fluctuations via the RANS approach [30]. The thermo-chemistry and turbulence properties calculated by the standard and modified EDC combustion models will be applied in the extinction models describing in sections 4.2 and 4.3.

4.2 EDC extinction model

It is well accepted that localized extinction occurs when the mixing time-scale becomes smaller than a typical chemical time-scale in the combustion process. According to this, the EDC combustion model cannot be employed directly to analyze local extinction. Since, if the residence time in the fine structure is too short, not only extinction occurs but also a fast chemistry will be approached according to Eq. (1). Therefore, neither versions of the EDC combustion model can be employed directly to predict local extinction by comparing of mixing and chemical time-scales.

In the EDC extinction model, however, a critical fine structure residence time is introduced which must always satisfy the energy and mass balance equations for the fine structure [31]. The fine structure mass balance is defined as:

$$Y_{fu} = \frac{R^*_{fu} \cdot \tau^*}{c^0_{fu}} \frac{\rho^0}{\rho^*} \tag{4}$$

where, R^*_{fu} is the rate of mass transfer between the fine structure and surrounding fluid and c^0_{fu} is the local concentration of the fuel in surrounding fluid. The EDC extinction model assumes that the rate of reaction between fuel and oxidizer is infinitely fast [31]. Hence, the rate of combustion is controlled by the mass transfer between the fine structure and surrounding fluid which is formulated as follows:

$$R^*_{fu} = \frac{\dot{m} \cdot \bar{c}_{\min}}{1 - \gamma^*} \qquad \left[\frac{kg}{m^3 \cdot s}\right] \tag{5}$$

where, $\bar{c}_{\min}$ is the smallest of local mean concentration of the fuel ($\bar{c}_{fu}$) and oxidizer ($\bar{c}_{O_2} / r_{fu}$) and r_{fu} is the stoichiometric O_2 requirement. $\dot{m}$ is the transfer rate of unit mass of fluid between the fine structure and surrounding which has been obtained based on turbulence parameters [31] as follows:

$$m = 23.6 \left(\frac{\nu \cdot \varepsilon}{k^2}\right)^{\frac{1}{4}} \cdot \frac{\varepsilon}{k} \qquad \left[\frac{1}{s}\right] \tag{6}$$

If fine structures are considered to be adiabatic, the fine structure energy balance can be defined as:

$$Y_{fu} = \frac{C_P \left(T^* - T^0\right) \rho^0}{\Delta H_R \cdot c^0_{fu}} \tag{7}$$

where, T^* and T^0 are the fine structure and surrounding fluid local temperatures, respectively. ΔH_R is, also, the heat of combustion generated in the fine structures. Thus, the critical fine structure residence time $\left(\tau^*_{cr}\right)$ which satisfies both heat and material balances can be derived from Eq. (4) and Eq. (7) as follows:

$$\tau_{cr}^{*} = \frac{C_P\left(T^{*} - T^{0}\right)\rho^{*}}{R_{fu}^{*} \cdot \Delta H_R} \qquad [s] \tag{8}$$

If the fine structure residence time defined in Eq. (3) becomes smaller than the critical residence time obtained in Eq. (8) reactions will not complete [31]. In other words, in fine structures with residence time smaller than τ_{cr}^{*} one of the mass or energy balance equations has not be satisfied resulting in extinction of chemical reactions in the fine structure.

4.3 Extended EDC extinction model

It is well accepted that in MILD conditions the chemical time-scale is of the same order of turbulent or mixing time-scale, leading to conditions far from the fast-chemistry assumption [32]. The aim of this section is to extend the applicability of the EDC local extinction model to the MILD combustion conditions by incorporating the effect of finite-rate chemistry in the rate of combustion reactions. The theoretical basis of model extension, here, will be discussed using two different perspectives, one based on diffusive fluxes and the other based on rate of reactions.

4.3.1 Diffusive perspective

According to Eq. (5) the rate of combustion reactions in the EDC extinction model is assumed to be controlled by the rate of mass transfer $\left(R_{fu}^{*}\right)$ from surrounding fluid to the fine structures [31]. Eq. (5) can be re-written using the molar flux of species *i* diffusing from surrounding fluid toward the fine structures as follows:

$$R_{fu}^{*} = \rho k_g \left(Y_i^0 - Y_i^1\right) \tag{9}$$

where, k_g is surrounding fluid mass transfer coefficient and Y_i^0 and Y_i^1 are the mass fraction of species *i* in surrounding fluid and at the fine structure entrance, respectively,

as schematically illustrated in Fig. 6a. Under the assumption of fast-chemistry, Y_i^1 can be assumed as Y_i^* resulting to development of the EDC extinction model [31] described in section 3.2. However, finite-rate effects may lead to deviation of Y_i^1 from Y_i^* (see Fig. 6b). According to the EDC combustion model [29] the source term in the conservation equation for the mean species *i* is modeled using Eq. (1). $\overline{R}_i = \frac{\gamma^{*2/3}}{\tau^*}\left(Y_i^* - Y_i^0\right)$As shown in Fig. 6b Y_i^0 at the fine structure entrance is denoted as $Y_i^1$to consider the effect of slow chemistry inside the fine structure. Therefore, another combustion resistance for the slow chemistry inside the fine structures could be defined as follows:

$$\overline{R}_i = \rho k_g^* \left(Y_i^* - Y_i^1\right) \tag{10}$$

where, k_g^* is the mass transfer coefficient inside the fine structures. Therefore, eliminating Y_i^1 between Eq. (9) and Eq. (10) will result in:

$$\begin{aligned} R_{new}^* &= \rho k_g \left(Y_i^0 - Y_i^* + \frac{\overline{R}_i}{\rho k_g^*} \right) \\ &= \rho k_g \left(Y_i^0 - Y_i^*\right) + \frac{k_g}{k_g^*}\overline{R}_i \end{aligned} \tag{11}$$

Since, temperature of the fine structures is, only, slightly higher than the surrounding or local mean temperature it can be assumed that k_g and k_g^* are almost equal. The fine structure temperature and local mean temperature of the HM1 and HM3 flames are depicted in Fig. 7. As can be seen in the contours of Fig. 7 the local mean and fine structure temperature fields are almost similar in both inner and outer regions of the flames. A more accurate comparison is shown in the X-Y plots of Fig. 7 where radial profiles of local mean and fine structure temperatures of both flames at to axial locations

297 are illustrated. It is observed that both temperature fields at two axial locations are quite
298 similar in fuel-rich and fuel-lean sides of the HM1 and HM3 flames. A minor deviation
299 is, however, observed at the peak temperatures which correspond to the main reaction
300 zones. Quantitatively speaking, the maximum values of local mean temperature at z = 30
301 mm from the burner tip are 1376.3 and 1718.3 K for HM1 and HM3 flames, respectively.
302 The corresponding maximum values for fine structure temperatures are 1433.5 and
303 1811.7 K. Similarly, at z = 120 mm from the burner tip the maximum values of local
304 mean temperatures are 1635.2 and 1874.8 K and the corresponding maximum fine
305 structure temperatures are 1756.2 and 2003.2 K for HM1 and HM3 flames, respectively.
306 These quantities reveal that deviation of local mean temperature from the fine structure
307 temperature in the main reaction zone is about 4 to 7 percent at all situations mentioned
308 above. As a consequence, the assumption of equal mass transfer coefficients at
309 surrounding and fine structure temperature fields could be reasonable. Therefore,
310 following to Eq. (11) a new definition for the rate of combustion reactions under the
311 effects of finite-rate chemistry is proposed as follows:

$$R^*_{new} = R^*_{fu} + \overline{R}_i \qquad (12)$$

312 where, R^*_{fu} is computed based on the Eq. (5) and $\overline{R}_i$ is the mean reaction rate of species *i*
313 in the fine structure computed using the EDC combustion model.

314 ***4.3.2 Reactive perspective***

315 Again, according to Eq. (5) the rate of combustion reactions in the EDC extinction
316 model is calculated based on a single-step mass transfer-controlled phenomenon leading
317 to the full equilibrium of $Y^*_{i,in}$ and $Y^*_{i,out}$ inside the fine structure (Fig. 6a). However, the
318 EDC combustion model can incorporate detailed chemistry into turbulent combustion to

account for finite rate effects. Based on Eq. (1) the concentration of specie *i* at the fine structure entrance $Y^*_{i,in}$ deviates from its outlet concentration $Y^*_{i,out}$ as they are not in equilibrium due to finite rate effects. In other words, in the EDC combustion model fine structures are assumed as partially stirred reactors which converts $Y^*_{i,in}$ to $Y^*_{i,out}$ with a finite rate of $\overline{R}_i$. To incorporate the effect of finite rate chemistry in the EDC extinction model we can start from the finite reaction rate available in the EDC combustion model and perform addition/subtraction of the inlet concentration:

$$\overline{R}_i = \frac{\gamma^{*2/3}}{\tau^*}\left(Y^*_{i,out} - Y^0_i\right) = \frac{\gamma^{*2/3}}{\tau^*}\left(Y^*_{i,out} - Y^0_i - Y^*_{i,in} + Y^*_{i,in}\right) \tag{13}$$

Rearranging above formula we have:

$$\begin{aligned} &\overline{R}_i = \frac{\gamma^{*2/3}}{\tau^*}\left(-Y^0_i + Y^*_{i,in}\right) + \frac{\gamma^{*2/3}}{\tau^*}\left(Y^*_{i,out} - Y^*_{i,in}\right) = -R^*_{fu} + R^*_{new} \\ &\Rightarrow R^*_{new} = R^*_{fu} + \overline{R}_i \end{aligned} \tag{14}$$

Eq. (14) is quite similar to Eq. (12) which was obtained based on the diffusive fluxes. Therefore, as shown in Fig. 6b, in the extended EDC extinction model proposed here based on diffusive and reactive viewpoints, besides the transfer rate of reactants from surrounding fluid to the fine structures $\left(R^*_{fu}\right)$, the rate of chemical reactions inside the fine structures $\left(\overline{R}_i\right)$ is incorporated to determine the overall rate of combustion. Hence, the new critical fine structure residence time is defined as follows:

$$\tau^*_{cr,new} = \frac{C_P\left(T^* - T^0\right)\rho^*}{R^*_{new} \cdot \Delta H_R} \qquad [s] \tag{15}$$

Based on the above new definition, the final expression for occurrence of local extinction in MILD conditions can be formulated as:

$$\lambda = \frac{\tau^*}{\tau^*_{cr,new}} \leq 1 \qquad (16)$$

In the proposed new extinction model the calculation of chemical time-scale is hidden in the determination of the mean reaction rate of species *i* in Eqs. (12) and (14) using the EDC combustion model. In addition, the extended EDC extinction model is applicable to both classical diffusion flames with $\overline{R}_i = 0$ (fast-chemistry assumption) in Eqs. (12) and (14), and newly developed MILD combustion flames. Last but not least, no ad-hoc constant parameters are employed in the new extinction model, extending its applicability to any kind of fuel.

5 Results and discussion

The implications of the extended EDC extinction model are now examined with the aid of the experimental observations of Dally et al. [22] and Medwell et al. [23] on the HM1 and HM3 flames of the JHC experiments reviewed in section 2. Moreover, the proposed new extinction model will be compared with the standard EDC extinction model on the prediction of extinction limits and position of the reaction zone. Here, we have focused on the HM1 and HM3 flames of the JHC experiments [22] which represent a MILD condition and flame-like behaviors, respectively. The flames conditions and their local extinction positions are presented in Table 2.

As can be seen in Table 2, while the jet Reynolds numbers are slightly different, in both experiments, the extinction was approached in HM1 flame at downstream. It arises from the fact that the reduced oxygen content in the oxidizer coflow at downstream can extinguish the weak HM1 flame. In addition, entraining more cooling air into the reaction zone can accelerate flame extinction at downstream [23].

From the numerical results (thermo-chemistry and turbulence parameters) obtained using the standard and modified EDC combustion models [19, 30], the local extinction criterion is, here, evaluated for the HM3 (flame-like behavior) and HM1 (MILD behavior) flames presented in Table 2. The resulting λ distributions are plotted in Figs. 8 and 9 against the mixture fraction calculated using the Bilger formula [26]. The local extinction analysis presented in Figs. 8 and 9 includes two extinction models that are:

1. The standard EDC extinction model: $\lambda = \tau^* / \tau_{cr}^* \leq 1$, where τ^* and τ_{cr}^* are defined based on Eq. (3) and Eq. (8), respectively.
2. The new extended EDC extinction model: $\lambda = \tau^* / \tau_{cr,new}^* \leq 1$, where τ^* and $\tau_{cr,new}^*$ are defined based on Eq. (3) and Eq. (15), respectively.

As mentioned above, to evaluate the role of turbulence-chemistry interaction model on the extinction analysis the above extinction models are examined based on the numerical results obtained using the standard and modified EDC combustion models [19]. As suggested by Medwell et al. [24], the reaction zone thickness (δ) was considered as the distance between the OH and CH_2O peaks which represent the fuel-lean and fuel-rich sides of the reaction zone, respectively. In Figs. 8 and 9, due to the steep distribution of λ across the main reaction zone, denoted by $\delta_{std.}$ and $\delta_{mod.}$ (obtained using the standard and modified EDC combustion models), part or the whole of the reaction zone may reach λ values below the limit as extinction approaches.

According to Table 2, no extinction has been observed for the HM3 flame at both upstream and downstream locations. The standard EDC extinction model coupled with the standard EDC combustion model completely failed to capture this behavior at upstream (z = 30 mm) as displayed in Fig. 8a. The extended EDC extinction model on

379 the same combustion field provides slightly improved results, but still half of the flame
380 predicted to be extinguished. The problem is solved when either the standard or extended
381 EDC extinction models have applied on the numerical solution obtained based on the
382 modified EDC combustion field (Fig. 8b). In other words, for the flame-like behavior of
383 HM3 flame the role of turbulence-chemistry interaction treatment on the accurate
384 prediction of local extinction is much more important than the direct role of the extinction
385 model. This issue supports the importance of previously proposed modification on the
386 treatment of turbulence-chemistry interaction in JHC flames [19].

387 At downstream (z = 120 mm), no extinction has been observed for the HM3 flame as
388 reported in Table 2. While the standard EDC extinction model was developed for the
389 classical combustion regimes which benefit an intense reaction zone, coupled with the
390 standard EDC combustion model it could not provide reasonable predictions for the HM3
391 flame at downstream (Fig. 8c). Even with the extended EDC extinction model on the
392 same combustion field the λ values, still, below the cross-over line for the entire reaction
393 zone. This failure is resolved when either the standard or extended EDC extinction
394 models were applied on the modified EDC combustion field (Fig. 8d). While the
395 extended EDC extinction model reveals reasonable results like the standard version, the
396 accurate resolving of turbulence-chemistry interaction using the modified EDC
397 combustion model shows superior influence on the extinction prediction for the HM3
398 flame.

399 To further evaluate the extended extinction model similar analysis is performed for
400 the HM1 flame. As illustrated in Fig. 9a, results of the standard and extended EDC
401 extinction models obtained on the standard EDC combustion field reveal total extinction

402 of the HM1 flame at 30 mm from the burner tip. This is against the experimental
403 observations on the HM1 flame in this position. However, by applying both standard and
404 extended EDC extinction models on the modified EDC combustion field (Fig. 9b) λ
405 values lie totally above the cross-over line in agreement with the experimental findings
406 that no extinction occurred at upstream of the HM1 flame.

407 According to the experimental observations presented in Table 2, HM1 flame partly
408 encountered to extinction at downstream. As can be seen in Fig. 9c and d only the new
409 extended EDC extinction model when applying on the numerical results obtained with
410 the modified EDC combustion model can predict this phenomenon properly. In relation
411 to the standard EDC extinction model, complete extinction of the HM1 flame across the
412 full extent of the reaction zone is thought to occur even when employed on the modified
413 EDC combustion field.

414 In general, it can be concluded that prediction of extinction limits in MILD conditions
415 is attainable only through the application of the new extended EDC extinction model on a
416 well resolved turbulence-chemistry interaction field.

417 Development of the extended EDC extinction model enables one to investigate the
418 influence of the amount of cooling air entrained into the reaction zone on the chemical
419 reaction rates. Fig. 10 illustrates the net reaction rate of CH_4 (as the bottleneck for
420 combustion reactions comparing with H_2) together with the available O_2 content at
421 different axial locations for the HM3 and HM1 flames. In Fig. 10 the HM3 and HM1
422 flames show a quite opposite manner along the axial direction. In HM3 flame, the net
423 reaction rate of methane is high at upstream and it decreases along the axial direction.
424 Conversely, for the HM1 flame the net reaction rate of methane close to the burner is low

and it increases toward downstream. This antithetical manner may be attributed to the competition between the oxygen penetrating from surrounding air to the reaction zone and its cooling effects on the flame. In the HM3 flame which benefits higher oxygen content in the hot coflow (9% by weight) a fixed amount of oxygen is available in the reaction zone along the axial distance, as can be seen in Fig. 10a. Therefore, penetrating surrounding air into the reaction zone at downstream, only, cools down the flame and resulted to slower methane oxidation in comparison with that at upstream. However, for the HM1 flame the oxygen deficient content in the hot coflow stream (3% by weight) slows down the methane reaction rate and resulted to partial extinction at upstream as previously captured by the proposed extended EDC extinction model. In addition, entraining more oxygen to the reaction zone towards downstream has accelerated methane oxidation as displayed in Fig. 10b. Interestingly, these specific behaviors of the JHC flames are captured by the proposed extension on the EDC extinction model and as shown previously resulted in accurate capturing of localized extinction for both HM3 and HM1 flames at upstream and downstream locations.

Despite the success in describing local extinction behavior of the Adelaide JHC flames, the extended EDC extinction model requires further tests and refinements to verify its wider applicability for other geometries, conditions and fuels.

6 Conclusions

In this paper, localized extinction is studied in the context of turbulent jet flames issuing into a heated and diluted coaxial oxidizer stream. A theoretical extension of the EDC extinction model was proposed to account the finite-rate chemistry effects normally occurs in MILD conditions, on the overall rate of combustion. According to this criterion

the flame is assumed to be locally extinguished, when the fine structure mixing time-scale is lower than a critical mixing time-scale determined in the present study. The proposed extinction model is evaluated against the experimental observations for JHC flames with 9% (HM3) and 3% (HM1) oxygen mass fraction in the hot coflow. It is found that, accurate prediction of flame extinction not only requires a reliable extinction model but also strongly dependent on the well treating of turbulence-chemistry interaction field. The presented local extinction model when applying on a well-resolved turbulence-chemistry interaction field is demonstrated to be able of capturing the local extinction behavior of purely MILD flames (HM1) as well as classical diffusion-like flames (HM3). Further investigations are needed to assess the suitability of the model for different types of flames.

References

[1] Kalghatgi GT. Liftoff heights and visible lengths of vertical turbulent jet diffusion flames in still air. Combust Sci Tech 1984;41:17–29.

[2] Takahashi F, Schmoll WJ, Trump DD, Goss LP. Vortex-flame interactions and extinction in turbulent jet diffusion flames. Proc Combust Inst 1996;26:145–152.

[3] Rolon JC, Aguerre F, Candel S. Experiments on the interaction between a vortex and a strained diffusion flame. Combust Flame 1995;100:422–429.

[4] Kim TH, Park J, Fujita O, Kwon OB, Park JH, Downstream interaction between stretched premixed syngas–air flames. Fuel 2013;104:739–748.

[5] Masri AR, Bilger RW, Dibbel RW. The local structure of turbulent nonpremixed flames near extinction. Combust Flame 1990;81:260–276.

[6] Masri AR, Dibble RW, Barlow RS. The structure of turbulent, nonpremixed flames revealed by Raman-Rayleigh-LIF measurements. Prog Energy Combust Sci 1996;22:307–326.

[7] Koutmos P. A Damkohler number description of local extinction in turbulent methane jet diffusion flames. Fuel 1999;78:623–626.

[8] Cavaliere A, de Joannon M. Mild combustion. Prog Energy Combust Sci 2004;30:329–366.

[9] Wünning JA, Wünning JG. Flameless oxidation to reduce thermal NO-formation. Prog Energy Combust Sci 1997;23:81–94.

[10] Tsuji H, Gupta AK, Hasegawa T, Katsuki M, Kishimoto K, Morita M. High temperature air combustion: from energy conservation to pollution reduction. New York: CRC;2003.

[11] Mastorakos E, Taylor AMKP, Whitelaw JH. Extinction of turbulent counterflow flames with reactants diluted by hot products. Combust Flame 1995;102:101–114.

[12] Maruta K, Muso K, Takeda K, Niioka T. Reaction zone structure in flameless combustion. Proc Combust Inst 2000;28:2117–2123.

[13] Kumar S, Paul PJ, Mukundar HS. Prediction of flame liftoff height of diffusion/partially premixed jet flames and modeling of MILD combustion burners. Combust Sci Tech 2007;179:2219–2253.

[14] Kumar S, Goel SK. Modeling of lifted methane jet flames in a vitiated coflow using a new flame extinction model. Combust Sci Tech 2010;182:1961–1978.

491 [15] Lilleberg B, Christ D, Ertesvåg IS, Rian KE, Kneer R. Numerical simulation with an
492 extinction database for use with the eddy dissipation concept for turbulent combustion.
493 Flow Turbul Combust 2013;91:319–346.
494 [16] Frassoldati A, Sharma P, Cuoci A, Faravelli T, Ranzi E. Kinetic and fluid dynamics
495 modeling of methane/hydrogen jet flames in diluted coflow. Appl Thermal Eng
496 2010;30:376–383.
497 [17] Vascellari M, Cau G. Influence of turbulence–chemical interaction on CFD
498 pulverized coal MILD combustion modeling. Fuel 2012;101:90–101.
499 [18] Lupant D, Lybaert P. Assessment of the EDC combustion model in MILD
500 conditions with in-furnace experimental data. Appl Thermal Eng 2015;75:93–102.
501 [19] Aminian J, Galletti C, Shahhosseini S, Tognotti L. Numerical investigation of a
502 MILD combustion burner, analysis of mixing field, chemical kinetics and turbulence-
503 chemistry interaction. Flow Turbul Combust 2012;88:597–623.
504 [20] De A, Oldenhof E, Sathiah P, Roekaerts D. Numerical simulation of Delft-jet-in-hot-
505 coflow (DJHC) flames using the Eddy Dissipation Concept model for turbulence-
506 chemistry interaction. Flow Turbul Combust 2011;87:537–567.
507 [21] Duwig C, Dunn MJ. Large Eddy Simulation of a premixed jet flame stabilized by a
508 vitiated co-flow: Evaluation of auto-ignition tabulated chemistry. Combust Flame
509 2013;160:2879–2895.
510 [22] Dally BB, Karpetis AN, Barlow RS. Structure of turbulent nonpremixed jet flames
511 in a diluted hot coflow. Proc Combust Inst 2002;29:1147–1154.

512 [23] Medwell PR, Kalt AM, Dally BB. Simultaneous imaging of OH, formaldehyde, and
513 temperature of turbulent nonpremixed jet flames in a heated and diluted coflow. Combust
514 Flame 2007;148:48–61.
515 [24] Medwell PR, Kalt AM, Dally BB. Reaction zone weakening effects under hot and
516 diluted oxidant stream conditions. Combust Sci Tech 2009;181:937–953.
517 [25] Pope SB. An explanation of the turbulent round jet/plane jet anomaly. AIAA J
518 1978;16:279–281.
519 [26] Bilger RW, Starner SH, Kee RJ. On reduced mechanism for methane-air combustion
520 in nonpremixed flames. Combust Flame 1990;80:135–149.
521 [27] McGee HA. Molecular engineering. New York:McGraw-Hill;1991.
522 [28] Magnussen BF. On the structure of turbulence and a generalized eddy dissipation
523 concept for chemical reactions in turbulent flow. in: 19th AIAA, Sc. Meeting, St. Louis,
524 USA;1981.
525 [29] Gran IR, Magnussen BF. A numerical study of a bluff-body stabilized diffusion
526 flame. Part 2. Influence of combustion modeling and finite-rate chemistry. Combust Sci
527 Tech 1996;119:191–217.
528 [30] Aminian J, Galletti C, Shahhosseini S, Tognotti L. Key modeling issues in
529 prediction of minor species in diluted-preheated combustion conditions. Appl Therm Eng
530 2011;31:3287–3300.
531 [31] Byggstøyl S, Magnussen BF. A model for flame extinction in turbulent flow. in: 4th
532 Symposium on Turbulent Shear Flows, Karsruhe, Germany;1983.

[32] Isaac BJ, Parente A, Galletti C, Thornock JN, Smith PJ, Tognotti L. A novel methodology for chemical time-scale evaluation with detailed chemical reaction kinetics. Energy Fuels 2013;27:2255–2265.

Table 1 Operating conditions of all three streams for the HM1 and HM3 flames [22]

	Fuel jet				Oxidant coflow					Tunnel air		
Flame	Q (kg/s)	T (K)	CH_4 (wt.%)	H_2 (wt.%)	u (m/s)	T (K)	O_2 (wt.%)	H_2O (wt.%)	CO_2 (wt.%)	u (m/s)	T (K)	O_2 (wt.%)
HM1	3.12e-4	305	88	11	3.2	1300	3	6.5	5.5	3.2	294	23.2
HM3	3.12e-4	305	88	11	3.2	1300	9	6.5	5.5	3.2	294	23.2

543
544
545 **Table 2** Flame conditions and the reported local extinctions

Flame	$YO_{2,coflow}$	T_{coflow}	Re_{jet}	Local extinction @ z = 30 mm	Local extinction @ z = 120 mm
HM1[a]	0.03	1300	10000	No	Yes
HM1[b]	0.03	1300	11000	No	Yes
HM3[a]	0.09	1300	10000	No	No
HM3[b]	0.09	1300	11000	No	No

546 [a]Dally et al. experiment [22], [b]Medwell et al. experiment [23]
547
548

549

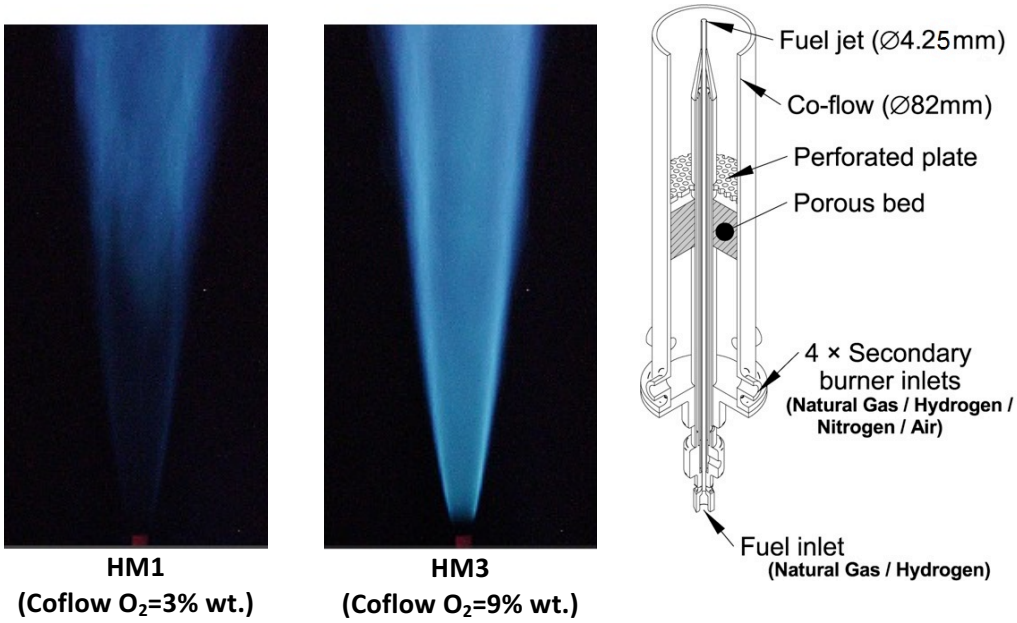

550

551 **Fig. 1** Jet-in-hot coflow burner configuration and hydrogen-methane flames [22]

552

553

554
555

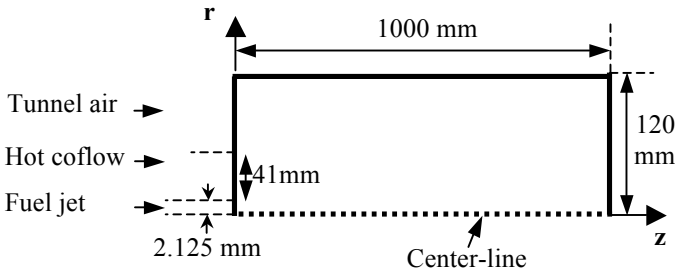

556
557 **Fig. 2** Computational domain with boundary conditions
558

559

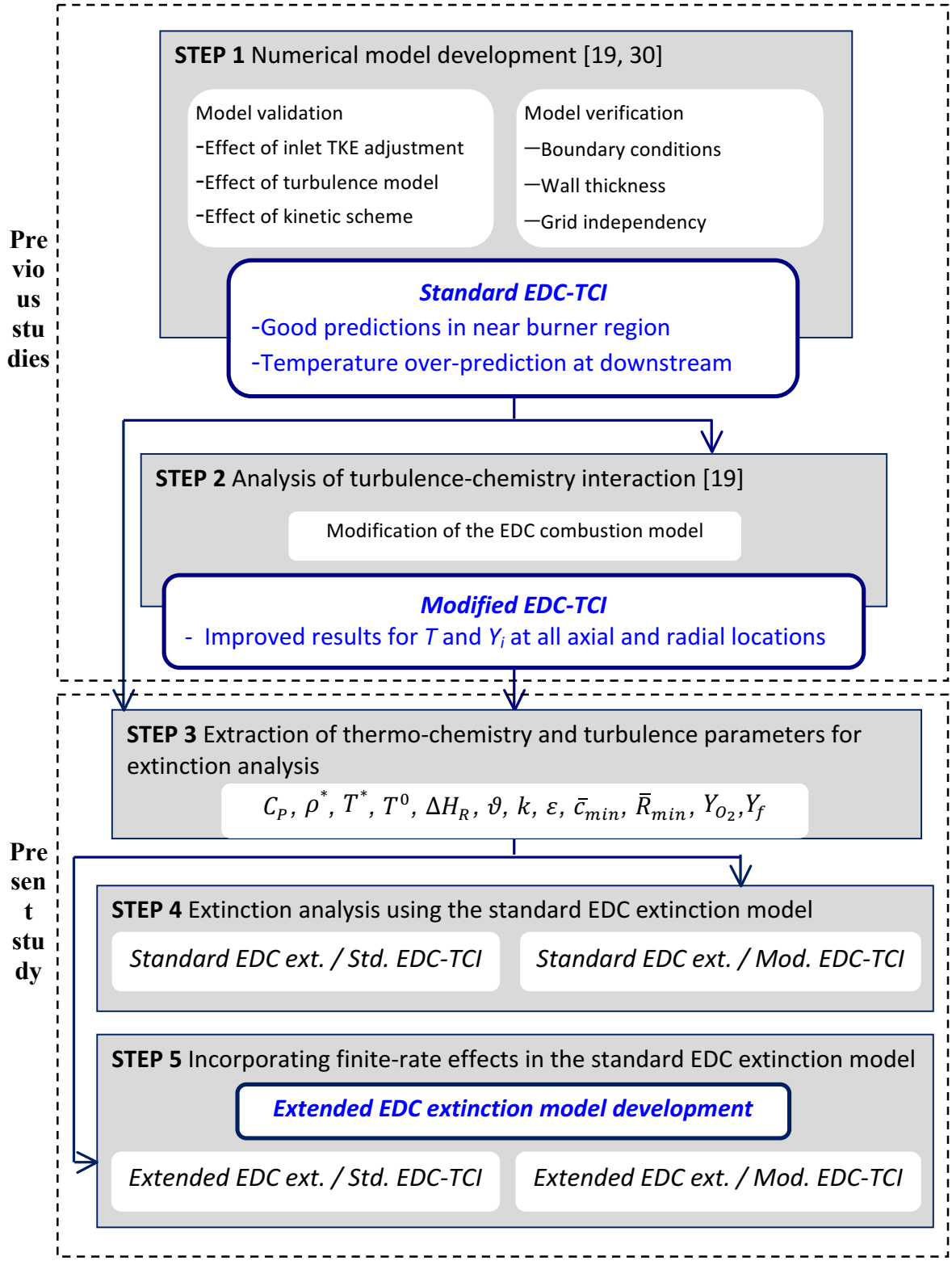

560

561 **Fig. 3** Conceptual scheme of the modeling strategy performed in previous studies (STEP 1 and STEP 2) for
562 modifying the EDC combustion model constant and the overall procedure of developing the extended EDC
563 extinction model in the present study (STEP 3 to STEP 5)

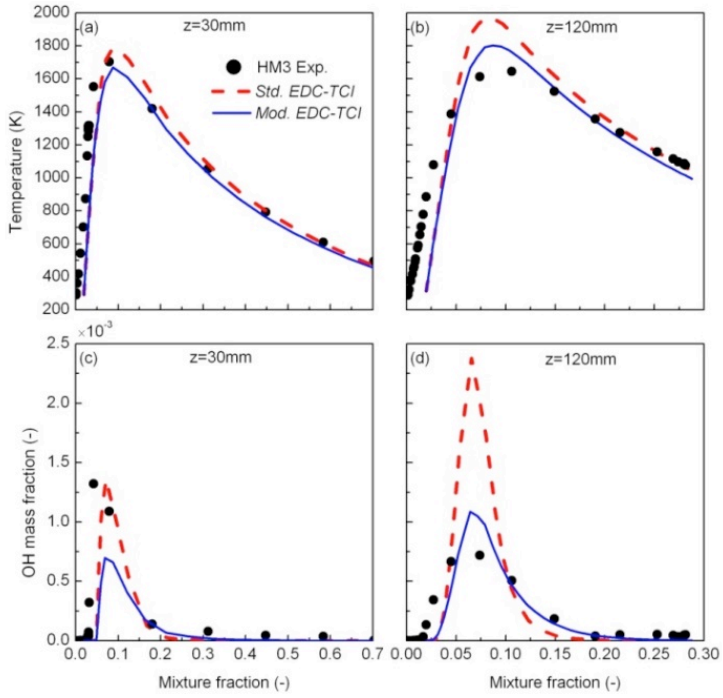

Fig. 4 Comparison of the standard (*Std.*) and modified (*Mod.*) EDC combustion models for prediction of temperature and hydroxyl profiles at two axial locations (z = 30 and 120 mm) for the HM3 (9% O_2 mass fraction in the hot coflow stream) flame [19]

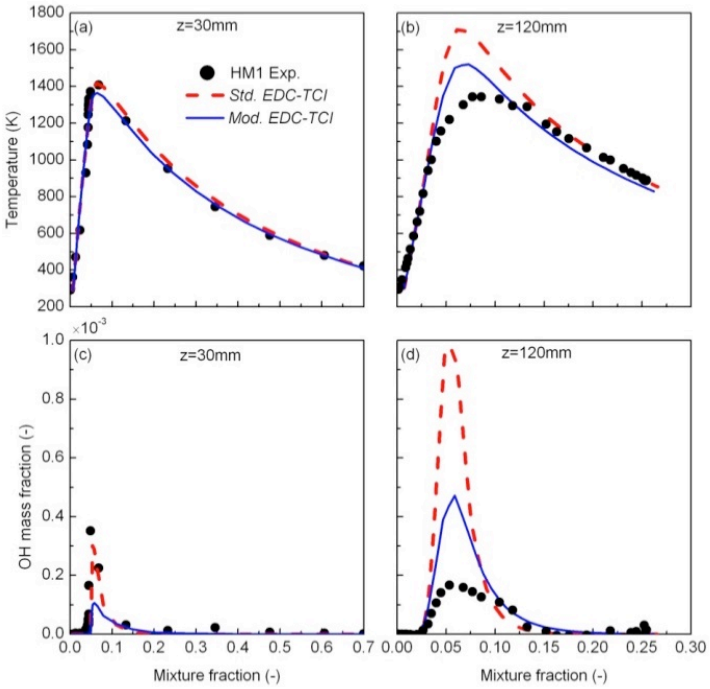

574

575 **Fig. 5** Comparison of the standard (*Std.*) and modified (*Mod.*) EDC combustion models for prediction of
576 temperature and hydroxyl profiles at two axial locations (z = 30 and 120 mm) for the HM1 (3% O_2 mass
577 fraction in the hot coflow stream) flame [19]

578

579

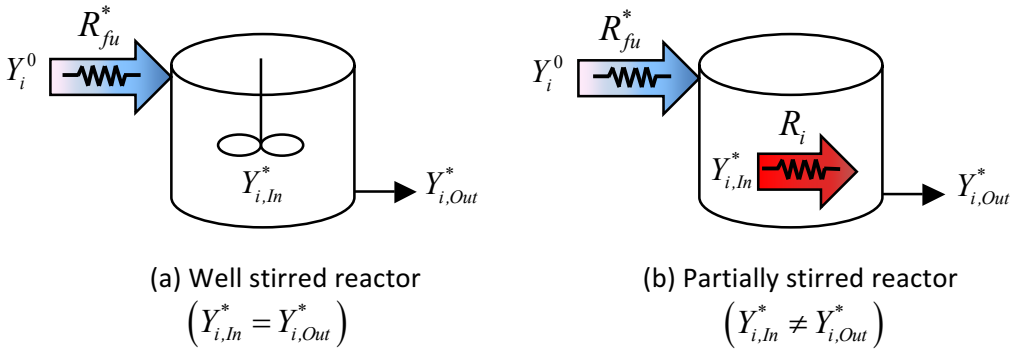

(a) Well stirred reactor $\left(Y^*_{i,In} = Y^*_{i,Out}\right)$

(b) Partially stirred reactor $\left(Y^*_{i,In} \neq Y^*_{i,Out}\right)$

Fig. 6 Schematic of combustion resistance(s) accounted for in a fine structure in the (left) standard EDC extinction model and (right) extended EDC extinction model

588

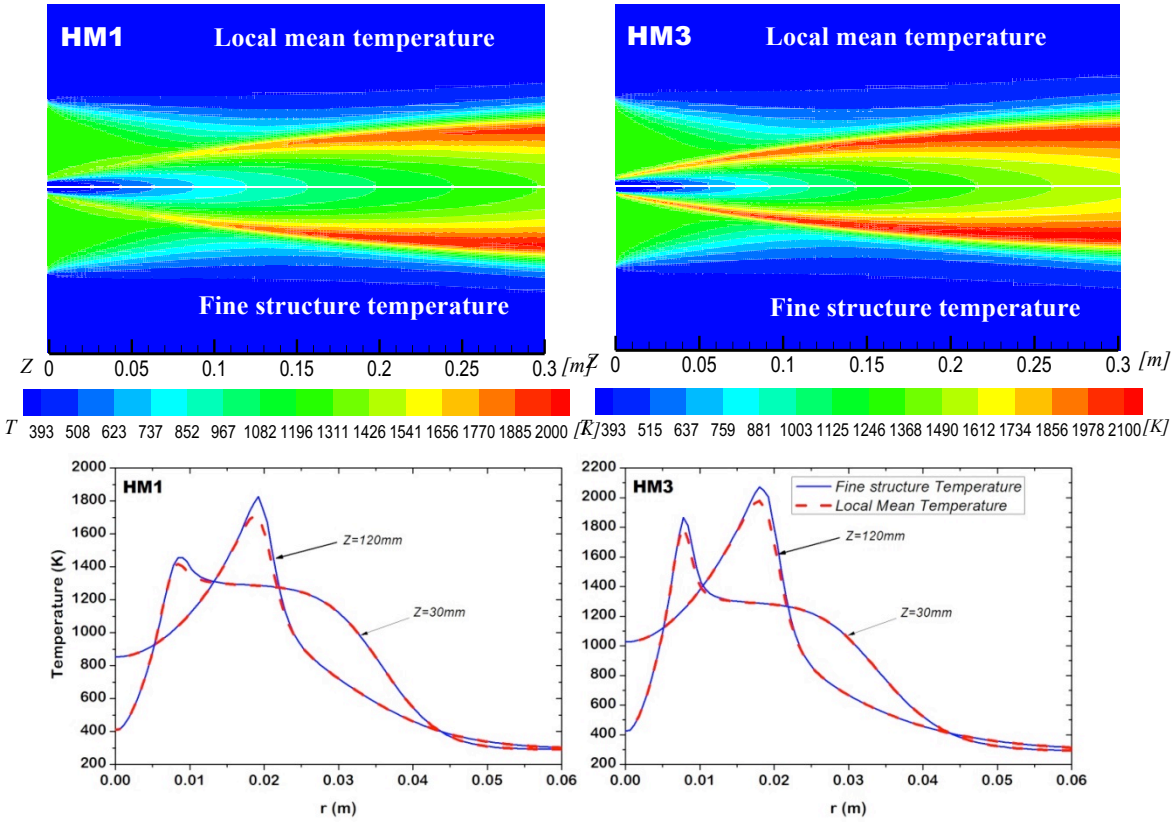

589 **Fig. 7** Comparison of fine structure and local mean temperature distributions in HM1 and HM3 flames

590

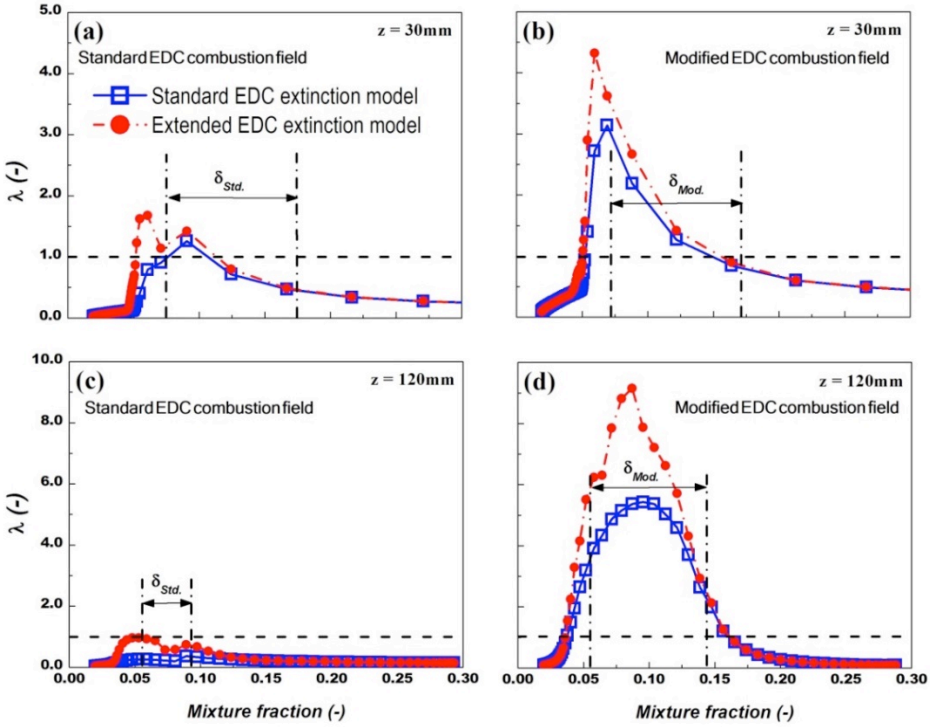

Fig. 8 Effect of extinction models combined with two versions of the EDC combustion model on local extinction analysis of the HM3 (9% O_2 mass fraction in the hot coflow stream) flame at two axial locations (z = 30 and 120 mm). The cross-over horizontal dashed line represents extinction limit in reaction zone below which extinction occurred.

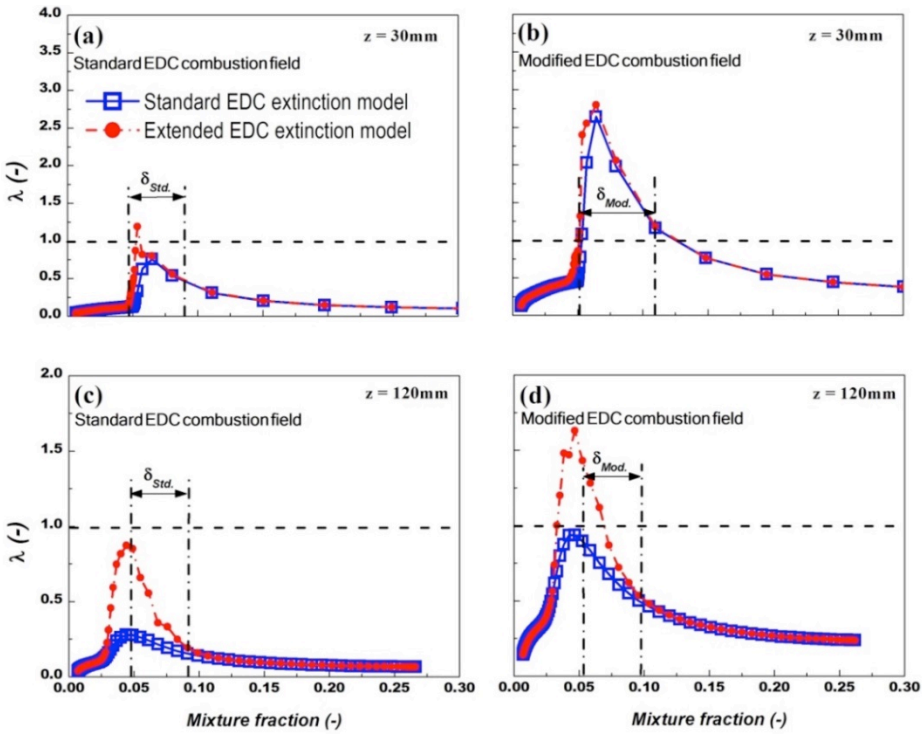

Fig. 9 Effect of extinction models combined with two versions of the EDC combustion model on local extinction analysis of the HM1 (3% O_2 mass fraction in the hot coflow stream) flame at two axial locations (z = 30 and 120 mm). The cross-over horizontal dashed line represents extinction limit in reaction zone below which extinction occurred.

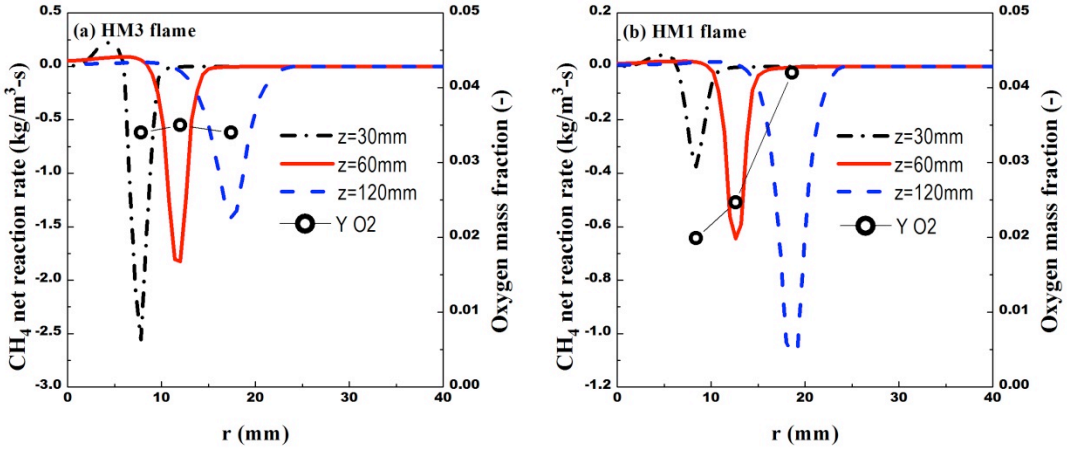

Fig. 10 Net reaction rate of methane and oxygen mass fraction in the reaction zone for HM3 and HM1 flames. First circle from left corresponds to axial location of z = 30 mm. Second circle corresponds to z = 60 mm and the third circle corresponds to axial location of z = 120 mm.